Acoustic anisotropy for acoustooptic $NaBi(MoO_4)_2$ crystals

Martynyuk-Lototska I., Mys O., Kushnirevych M., Krupych O. and Vlokh R.

Vlokh Institute of Physical Optics, 23 Dragomanov Street, 79005 Lviv, Ukraine

Received: 17.02.2015

Abstract. Basing on the comprehensive studies of acoustic properties for $NaBi(MoO_4)_2$ crystals, we have determined the full matrices of elastic stiffness and compliance coefficients and constructed cross sections of acoustic-wave velocity surfaces by the principal crystallographic planes. We have shown that the slowest acoustic wave propagates in the *ab* plane at the angle 61.9 deg with respect to the *a* axis and has the velocity ~ 1948 m/s. The interaction with that wave is expected to provide the highest acoustooptic figure of merit. Deviations of polarization states of the acoustic waves from the purely longitudinal and transverse types and deviations of the acoustic energy flux from the wave vector direction are analyzed for the $NaBi(MoO_4)_2$ crystals.

Keywords: acoustic wave velocities, elastic stiffness, elastic compliance, anisotropy

PACS: 42.79.Jq, 43.35.Sx
UDC: 535.012.2+535.42+534.321.9

1. Introduction

$NaBi(MoO_4)_2$ crystals represent a scheelite family [1] and originate from a calcium tungstate mineral with the chemical formula $CaWO_4$ [2]. The scheelite crystals, which are named after Swedish chemist Karl Wilhelm Scheele, are most often tetragonal and belong to dipyramidal or pseudo-octahedral types. Under normal conditions, double sodium-bismuth molibdate crystals are described by the tetragonal point symmetry group 4/m [3]. Their unit cell contains two formula units and the cell parameters are equal to $a = b = 0.5274$ nm and $c = 1.1578$ nm [3]. The crystals are interesting from the viewpoints of their acoustooptic (AO) properties [4] and structural transformations [3, 5].

Recently a second-order ferroelastic phase transition (PT) with the change of spatial symmetry $I4_1/a\,F\,I2_1/a$ has been reported for the $NaBi(MoO_4)_2$ crystals at $T_C = 241$ K, basing on the X-ray measurements and the detection of domain structure below T_C [3]. This PT is accompanied by the appearance of shear strains of their unit cell in the crystallographic plane *ab* of tetragonal lattice set and by small displacements of Na^+ and Bi^{3+} cations from their high-symmetry positions [3]. As a result, the PT in $NaBi(MoO_4)_2$ seems to be of a displacement type. If to follow from the data of work [3] and considering the symmetry change and the type of PT, one can regard it to be analogical to that occurring in $BiVO_4$ crystals [6–8]. However, the need of application of procedure of crystallographic axes replacement [3] for PT description in the $NaBi(MoO_4)_2$ crystal, seems unclear. Notice that the last fact may be associated with the improper character of the PT.

Notice that, in the case of proper PT the acoustic phonon softens notably and so the appropriate acoustic wave (AW) velocity and the effective elastic stiffness coefficient approach zero in the close vicinity of the PT point [9]. More specifically, the PT in $BiVO_4$ is driven by softening of the transverse acoustic phonon with the wave vector lying in the plane (001) at the

angle of 55 deg with respect to the [100] direction, whereas its polarization belongs to the same plane. The velocity of the acoustic phonon acquires a minimum (~ 300 m/s) at T_C, although this velocity remains as high as 1800 m/s at the room temperature [10, 11]. The AO figure of merit (AOFM) estimated for the interaction with this type of AW can be high enough (3400×10^{-15} s^3/kg [12]). It is interesting that, even for the much less favourable case of AO interaction with the longitudinal AW (the velocity $v_{33} = 3990$ m/s and the propagation direction [001]), the AOFM for $BiVO_4$ remains not so low (415×10^{-15} s^3/kg [13]).

We remind that the AOFM is determined by the formula $M_2 = n^6 p_{ef}^2 / \rho v_{ij}^3$, with n being the refractive index, p_{ef} the effective elastooptic coefficient, ρ the density of material, v_{ij} the velocity of AW taking part in the AO interaction, and the indices i and j corresponding to the directions of wave propagation and polarization of the AW, respectively. It is obvious that the AOFM depends significantly upon the AW velocity. Therefore the AOFM of $NaBi(MoO_4)_2$ crystals can prove to be high enough, since the AW velocity for the mode conjugated with the soft acoustic phonon can become very low both in the vicinity of the PT and under the normal conditions.

The AW velocities for the $NaBi(MoO_4)_2$ crystals have been studied well under the normal conditions [14]. It has been found that the slowest AW is a transverse mode propagating in the *ab* plane at the angle of 63.1 deg with respect to the *a* axis. It is polarized in the same plane [14]. The velocity of this wave calculated from the data of Ref. [14] at 293 K is approximately equal to 2077 m/s (or 1903 m/s when calculating with the data of Ref. [15]). The AO interaction with this slow wave can lead to essential increase in the AOFM. Moreover, one can expect that this acoustic mode should behave as a soft mode, i.e. its frequency should tend to zero when approaching the Curie temperature and its velocity has to decrease. This would lead to additional increase in the AOFM.

In other words, the AO efficiency of $NaBi(MoO_4)_2$ could be strongly linked to the ferroelastic PT. Notice that the temperature dependences of the AW velocities for the $NaBi(MoO_4)_2$ crystals have not yet been studied in the course of the PT. Among the other parameters needed for calculating the AOFM [16], there are the refractive indices and the elastooptic coefficients. The refractive indices for the optically negative $NaBi(MoO_4)_2$ crystals are known to be equal to $n_o = 2.295$ and $n_e = 2.198$ at the wavelength of 633 nm [15]. Only some of the elastooptic coefficients have been determined up to date. These are $p_{33} = 0.29$, $p_{13} = 0.25$, $p_{31} = 0.21$, $p_{21} = 0.205$, and $p_{11} = 0.243$ [4]. The AOFM value obtained in the work [4] is not so high (less than $\sim 24\times10^{-15}$ s^3/kg), in spite of the fact that the elastooptic coefficients are high enough. This means that the AO interaction occurs with rather fast AWs.

As a consequence, the present work begins comprehensive studies of the acoustic and elastooptic properties of $NaBi(MoO_4)_2$ crystals under the normal conditions and in the course of their phase transition. The main aim is to find the optimal conditions of AO interactions. In particular, we will present the results for acoustic and elastic anisotropies for the $NaBi(MoO_4)_2$ crystals and will estimate the AOFM that can be reached during AO interactions with the slowest AW.

2. Experimental methods and results

We prepared six samples of $NaBi(MoO_4)_2$ with the faces perpendicular to the crystallographic directions [100], [001], [110], [2 $\bar{1}$ 0], [120], [210], [1 $\bar{2}$ 0] and to the vector defined by the directional cosines $\left(0;1/\sqrt{2};1/\sqrt{2}\right)$. The thicknesses along the directions of AW propagations were equal to 2–6 mm. The AWs were excited with a piezoelectric $LiNbO_3$ transducer at the

frequency of 10 MHz (the bandwidth $\Delta f = 0.1$ MHz and the acoustic power $P_a = 1-2$ W). The AW velocity was measured at the temperature $T = 293$ K, using a well-known pulse-overlap method [17]. Direct and simple relations among the velocities measured and the elastic stiffness coefficients exist only for the two of the elastic stiffness matrix components ($C_{33} = \rho v_{33}^2$ and $C_{44} = \rho v_{31}^2 = \rho v_{32}^2 = \rho v_{13}^2 = \rho v_{23}^2$). All the other five coefficients are linked by much more complicated relations [18]. Finally, the matrix of elastic compliances was calculated as a reciprocal of the matrix of elastic stiffnesses.

Table 1. AW velocities for $NaBi(MoO_4)_2$ crystals measured at $T = 293$ K.

Type and notation of AW *	Wave vector direction	Displacement direction	AW velocity, m/s
QL, v_{11}	[100]	[100]	4337±9
QT, v_{12}	[100]	[010]	2511±7
T, v_{13}	[100]	[001]	2113±7
T, v_{31}	[001]	[100]	2122±7
T, v_{32}	[001]	[010]	2115±7
L, v_{33}	[001]	[001]	3982±9
QL, v_{66}	[110]	[110]	4569±7
QT, $v_{6\,\bar{6}}$	[110]	$[1\,\bar{1}0]$	2323±7
T, v_{63}	[110]	[001]	2106±7
QL, $v_{\bar{6}*\bar{6}*}$	$[2\,\bar{1}0]$	$[2\,\bar{1}0]$	4652±21
QT, $v_{\bar{6}*6*}$	$[2\,\bar{1}0]$	[120]	1889±28
T, $v_{\bar{6}*3}$	$[2\,\bar{1}0]$	[001]	2110±7
QL, v_{6*6*}	[120]	[120]	4610±21
QT, $v_{6*\,\bar{6}*}$	[120]	$[2\,\bar{1}0]$	1834±28
T, v_{6*3}	[120]	[001]	2121±7
QL, $v_{6^\times 6^\times}$	[210]	[210]	4300±18
QT, $v_{6^\times\bar{6}^\times}$	[210]	$[1\bar{2}0]$	2615±22
T, $v_{6^\times 3}$	[210]	[001]	2111±7
QL, $v_{\bar{6}^\times\bar{6}^\times}$	$[1\bar{2}0]$	$[1\bar{2}0]$	4265±18
QT, $v_{\bar{6}^\times 6^\times}$	$[1\bar{2}0]$	[210]	2658±22
T, $v_{\bar{6}^\times 3}$	$[1\bar{2}0]$	[001]	2101±7
QL, v_{44}	$\left(0;1/\sqrt{2};1/\sqrt{2}\right)$ **	$\left(0;1/\sqrt{2};1/\sqrt{2}\right)$ **	4038±9
QT, $v_{4\,\bar{4}}$	$\left(0;1/\sqrt{2};1/\sqrt{2}\right)$ **	$\left(0;1/\sqrt{2};-1/\sqrt{2}\right)$ **	2451±7
T, v_{41}	$\left(0;1/\sqrt{2};1/\sqrt{2}\right)$ **	[100]	2193±7

* L denotes pure longitudinal, T pure transverse, QL quasi-longitudinal and QT quasi-transverse waves; ** these are directional cosines.

The AW velocities for the $NaBi(MoO_4)_2$ crystals are presented in Table 1. The slowest wave detected experimentally propagates along the direction [120]. It is polarized parallel to the $[2\bar{1}0]$ direction and the velocity of 1834±28 m/s. Almost the same velocity (1889±28 m/s) has been obtained for the AW that propagates along the direction $[2\bar{1}0]$ and has polarization parallel to [120]. Notice that these represent the same waves and their mean velocity equals to 1861±28 m/s. They are the slowest AWs in $NaBi(MoO_4)_2$.

3. Discussion

The elastic stiffness and compliance coefficients calculated by us are presented in Table 2 and Table 3, respectively. Our data agree well with the results of the earlier works. Note that a nonzero coefficient C_{16} is responsible for rotation of the indicative surface of elastic stiffness coefficients (or of the AW velocity surface) around the crystallographic axis *c*. The rotation angle is given by [19]

$$\varphi_C = 0.25 \arctan\left[\frac{4C_{16}}{C_{11} - C_{12} - 2C_{66}}\right]. \quad (1)$$

Hence, the coordinate eigensystem $a'b'c$ of the elastic stiffness tensor for $NaBi(MoO_4)_2$ is rotated by 16.9 deg around the *c* axis. The elastic stiffness coefficients rewritten in that coordinate system are as follows: $C'_{16} = 0$, $C'_{12} = 55.08\times10^9$, $C'_{11} = 98.27\times10^9$ and $C'_{66} = 44.63\times10^9$ N/m^2. In other words, the coefficients C'_{12}, C'_{11} and C'_{66} differ respectively from C_{12}, C_{11} and C_{66} by ~ 7–16%.

Table 2. Elastic stiffness coefficients for $NaBi(MoO_4)_2$ crystals calculated in the units of 10^9N/m^2.

C_{11}	C_{12}	C_{13}	C_{16}	C_{33}	C_{44}	C_{66}	Ref.
107.63±0.12	51.66±0.12	33.42±0.15	–10.12±0.10	88.14±0.10	25.36±0.08	34.45±0.08	[15]
104.9±0.5	45.1±0.5	37.3±0.5	–7.2±1.0	78.6±0.2	25.4±0.1	34.5±0.5	[14]
105.40±0.33	47.96±15.84	35.58±1.41	–10.64±1.07	90.22±0.41	25.40±0.07	37.51±0.33	Present work

Table 3. Elastic compliance coefficients of $NaBi(MoO_4)_2$ crystals calculated in the units of 10^{-12} m^2/N.

S_{11}	S_{12}	S_{13}	S_{16}	S_{33}	S_{44}	S_{66}	Ref.
13.728	–6.262	–2.831	5.872	13.492	39.432	32.478	[15]
13.167	–4.441	–4.141	3.675	16.653	39.370	30.519	[14]
13.7±2.5	–5.7±3.5	–3.15±0.44	5.5±1.8	13.57±0.40	39.37±0.11	29.8±1.2	Present work

Using the Christoffel equation [20] and our elastic stiffness data, we have constructed cross sections of the AW velocity surfaces by the principal crystallographic planes (see Fig. 1). As seen from Fig. 1, the slowest of the QT_1 waves propagates in the *ab* plane at the angle 61.9 deg with respect to the *a* axis (the velocity ~ 1948 m/s). The lowest velocity for the QT_2 waves (2113 m/s) is reached for the propagation directions parallel to the crystallographic axes or those lying in the *ab* plane. Finally, the QL waves reveal the minimal velocity (3982 m/s) whenever the propagation direction is parallel to the *c* axis.

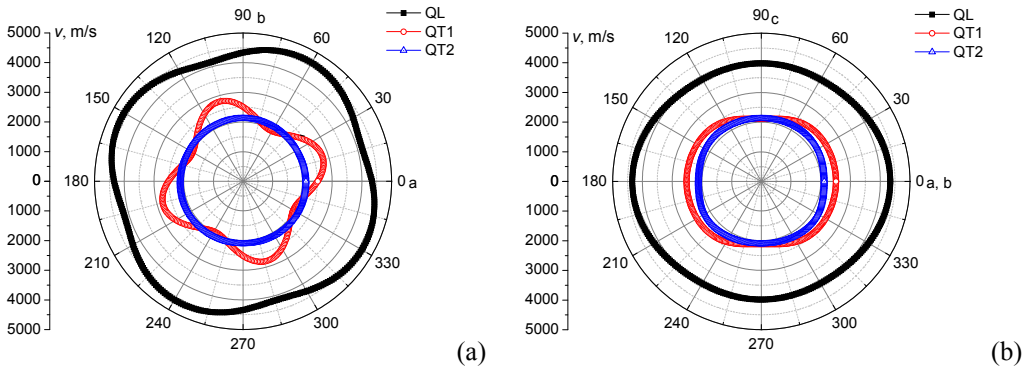

Fig. 1. Cross sections of AW velocity surfaces by the crystallographic planes *ab* (a), *ca* and *cb* (b).

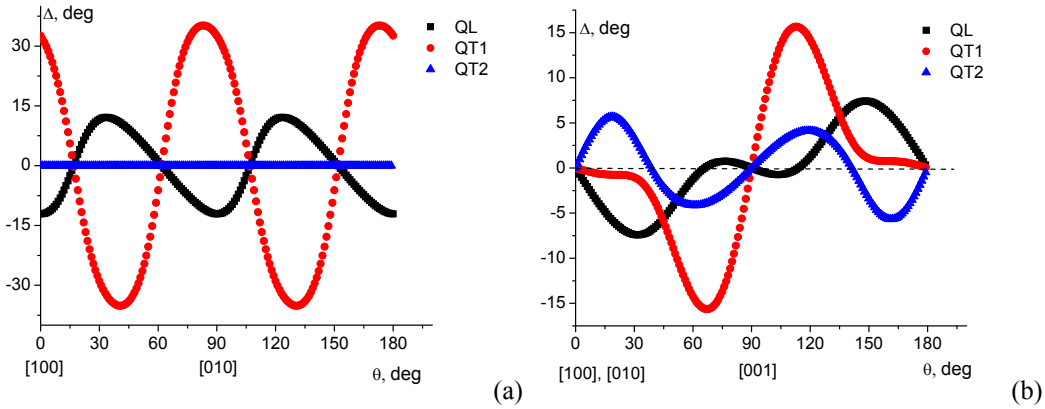

Fig. 2. Dependences of obliquity angle on the wave vector orientation in the crystallographic planes *ab* (a), *ac* and *bc* (b).

The angle of obliquity of the acoustic energy flux with respect to the AW wave vector can be calculated from the relation [20]

$$\Delta = \arctan\left[\frac{1}{v(\theta)}\frac{dv}{d\theta}\right], \tag{2}$$

where θ implies the angle between the AW wave vector and the corresponding crystallographic axis. The maximal deviation of the acoustic energy flux from the direction of the wave vector (~ 35 deg) is peculiar for the QT_1 wave propagating in the *ab* plane at the angles 41, 83, 131 and 173 deg with respect to the *a* axis (Fig. 2). For the other waves this angle does not exceed ~ 7.4 deg. It is interesting that the QT_2 wave exhibits no velocity anisotropy and its obliquity angle in the crystallographic plane *ab* remains zero.

The dependences of deviation angle between the displacement vector and the direction of the wave vector (see Fig. 3) can be calculated using the following equations:

$$\Delta\xi = 0.5\arctan\left[\tan(2\theta)\frac{C_{12}+C_{66}}{C_{11}-C_{66}}\right] \tag{3}$$

for the $a'b'$ plane,

$$\Delta\xi = 0.5\arctan\left[\frac{\sin(2\theta)(C_{13}+C_{44})}{(C_{11}-C_{44})\cos^2(\theta)+(C_{44}-C_{33})\sin^2(\theta)}\right] \tag{4}$$

for the $a'c$ plane, and

$$\Delta\xi = 0.5\arctan\left[\frac{\sin(2\theta)(C_{13}+C_{44})}{(C_{11}-C_{44})\cos^2(\theta)+(C_{44}-C_{33})\sin^2(\theta)}\right] \tag{5}$$

for the $b'c$ plane.

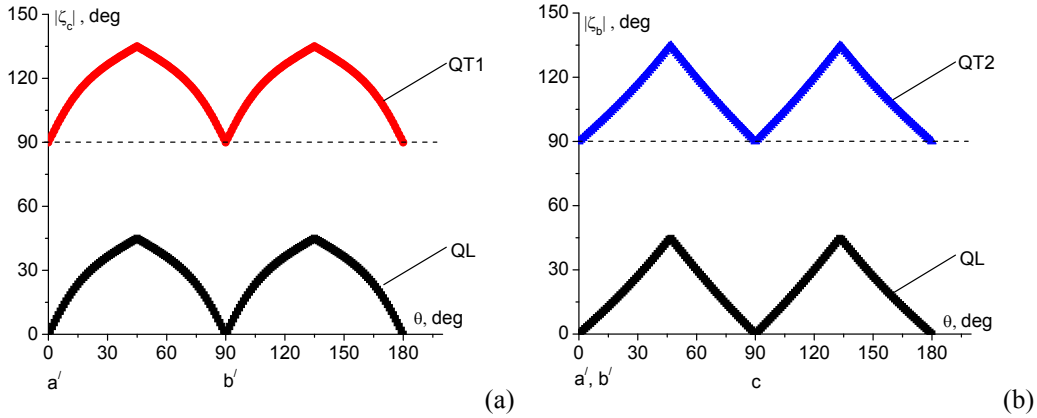

Fig. 3. Deviation angle between the displacement vector and the wave vector in the planes $a'b'$ (a), $a'c$ and $b'c$ (b) of the coordinate eigensystem $a'b'c$.

The deviation of acoustic polarization from the purely longitudinal and transverse types reaches its maximal value equal to 45 deg in the cases when the QL and QT_1 waves propagate in the $a'b'$ plane along the bisectors of the a' and b' axes, respectively. When the QL and QT_2 waves propagate in the $a'c$ and $b'c$ planes at the angle of 47 deg with respect to the a' and b' axes, their polarization deviates by 44.6 deg from the purely longitudinal or transverse types.

Now let us analyze the possible AO interactions with the slowest AWs in the $NaBi(MoO_4)_2$ crystals and the corresponding AOFM values, issuing from the data available for the elastooptic coefficients [4]. Below we will restrict our consideration to the isotropic AO interactions in the principal crystallographic plane *ab* and the polarizations of the incident and diffracted optical waves belonging to the same *ab* plane. Then the effective elastooptic coefficient for the incident optical wave polarized along the *c* axis is zero. The effective elastooptic coefficient in this case may be written as follows:

$$\begin{aligned} p_{ef} &= \cos 2(\theta_B+\Theta)\left[0.5(p_{11}-p_{12})\sin 2\Theta + p_{16}\cos 2\Theta\right] \\ &+ \sin 2(\theta_B+\Theta)\left[p_{61}\sin 2\Theta + p_{66}\cos 2\Theta\right], \end{aligned} \tag{6}$$

where θ_B is the Bragg angle and Θ the angle of the AW propagation with respect to the *a* axis. As readily seen from Eq. (6), the parameter p_{ef} contains the elastooptic coefficients p_{16} and p_{66}, which are unknown. As a consequence, we cannot estimate the effective elastooptic coefficient and the AOFM, even roughly. Nonetheless, the characteristics of $NaBi(MoO_4)_2$ considered here are promising enough to suspect that it can well prove an efficient AO material. The studies of the relevant elastooptic coefficients will be reported in our forthcoming works.

4. Conclusions

Basing on our comprehensive studies of the acoustic properties of $NaBi(MoO_4)_2$, we have determined the full matrices of the elastic stiffness and compliance coefficients. Our results agree

well with the known literature data. The cross sections of the AW velocity surfaces by the principal crystallographic planes have been constructed. We have shown that the slowest principal AW QT_1 propagates in the *ab* plane at 61.9 deg with respect to the *a* axis and has the velocity ~ 1948 m/s. The smallest velocity for the QT_2 waves (2113 m/s) is peculiar for the propagation direction parallel to the crystallographic axes or, alternatively, for the directions lying in the *ab* plane. The QL waves acquire a minimal velocity (3982 m/s) when propagating along the *c* axis.

We have also found that the maximal deviation from the longitudinal and transverse AW types, ~ 45 deg, is reached for all the waves propagating in the vicinity of bisectors of the crystallographic axes. The maximal deviation of the acoustic energy flux from the wave vector direction, ~ 35 deg, is peculiar for the QT_1 wave propagating in the *ab* plane at the angles 41, 83, 131 and 173 deg with respect to the *a* axis. This angle does not exceed ~ 7.4 deg for the other waves. It is also interesting that the QT_2 wave does not exhibit anisotropy of the velocity and its obliquity in the *ab* crystallographic plane is zero. Finally, we have stated that, in order to calculate consistently the AOFM for the $NaBi(MoO_4)_2$ crystals for the cases of AO interactions with the slowest AWs, the values of all the elastooptic coefficients are needed.

References

1. Sillen L G and Sundvall H, 1943. Double molybdates and tungstates of alkali metals. Arkiv kemi, mineralogi och. geol. **A17:** 1–18.
2. Hazen R M, Finger L W and Mariathasan J W E, 1985. High-pressure crystal chemistry of scheelite-type tungstates and molybdates. J. Phys. Chem. Solids. **46**: 253–263.
3. Wasrkowska A, Gerward L, Staun Olsen J, Maczka M, Lis T, Pietraszko A and Morgenroth W, 2005. Low-temperature and high-pressure structural behaviour of $NaBi(MoO_4)_2$ – an X-ray diffraction study. J. Sol. State Chem. **178**: 2218–2224.
4. Akimov S V, Stolpakova T M, Dudnik E F and Sinyakov E V, 1977. Photoelastic properties of $NaBi(MoO_4)_2$. Fiz. Tverd. Tela. **19**: 1832–1833.
5. Pelikh L N and Gurskas A A, 1979. Low temperature paraelectric $NaBi(MoO_4)_2$. Fiz. Tverd. Tela **21**: 218–219.
6. David W I F, Glazer A M and Hewat A W, 1979. The structure and ferroelastic phase transition of $BiVO_4$. Phase Trans. **1**: 155–170.
7. Wood I G and Glazer A M, 1980. Ferroelastic phase transition in $BiVO_4$ I. Birefringence measurements using the rotating analyser method. J. Appl. Cryst. **13**: 217–223.
8. Wood I G, Welber B, David W I F and Glazer A M, 1980. Ferroelastic phase transition in $BiVO_4$ II. Birefringence at simultaneous high pressure and temperature. J. Appl. Cryst. **13**: 224–229.
9. David W I F, 1983. Ferroelastic phase transition in $BiVO_4$: III.Thermodynamics. J. Phys. C: Solid State Phys. **16**: 5093–5118.
10. Pinczuk A, Burns G and Dacol F H, 1977. Soft optical phonon in ferroelastic $BiVO_4$. Sol. State Commun. **24**: 163–165.
11. Avakyants L P, Dudnik E F, Kiselyov L F and Mnushkina I E 1983. Study of the soft acoustic mode in ferroelastic $BiVO_4$. Fiz. Tv. Tela, **25**: 1910–1912.
12. Vlokh R and Martynyuk-Lototska I, 2009. Ferroelastic crystals as effective acoustooptic materials. Ukr. J. Phys. Opt. **10**: 89–99.
13. Akimov S V, Mnushkina I E and Dudnik E F, 1982. Acoustooptic parameters of the bismuth vanadate. Zhurn. Tekhn. Fiz. **52**: 784–785.

14. Antonenko A M and Stolpakova T M, 1984. Acoustic properties of the $NaBi(MoO_4)_2$ crystals. Ukr. Fiz. Zhurn. **29**: 612–614.
15. Haussühl S, Liebertz J and Schmidt H, 1991. Crystal growth and elastic properties of tetragonal $NaBi(MoO_4)_2$. Cryst. Res. Technol. **26**: K136–K140.
16. Mys O, Kostyrko M, Smyk M, Krupych O and Vlokh R, 2014. Anisotropy of acousto-optic figure of merit in optically isotropic media. Appl. Opt. **53**: 4616–4627.
17. Papadakis E P, 1967. Ultrasonic phase velocity by the pulse-echo-overlap method incorporating diffraction phase corrections. J. Acoust. Soc. Amer. **42**: 1045–1051.
18. Chung D Y and Li Y, 1971. Ultrasonic wave propagation in tetragonal crystals and measurements of the elastic constants of strontium molibdate. Phys. Stat. Sol. (a). **5**: 669–675.
19. Farley J M, Saunders G A and Chung D Y, 1973. The elastic constants of strontium molibdate. J. Phys. C: Solid State Phys. **6**: 2010–2019.
20. Sirotin Yu I and Shaskolskaya M P, Fundamentals of crystal physics. Moscow: Nauka, (1979).

Martynyuk-Lototska I., Mys O., Kushnirevych M., Krupych O. and Vlokh R. 2015. Acoustic anisotropy for acoustooptic $NaBi(MoO_4)_2$ crystals. Ukr.J.Phys.Opt. **16**: 69 – 76.

Анотація. *На основі всебічного вивчення акустичних властивостей кристалів $NaBi(MoO_4)_2$ визначено всі коефіцієнти матриць пружних модулів і податливостей і побудовано перетини поверхонь швидкостей акустичних хвиль кристалографічними площинами. Встановлено, що найповільніша акустична хвиля поширюється в площині ab під кутом 61.9 град до осі a зі швидкістю ~ 1948 м/с. Взаємодіє з нею дає змогу очікувати найвищого значення коефіцієнта акустооптичної якості. Проаналізовано відхилення вектора акустичного зміщення від поздовжнього і поперечного станів поляризації акустичних хвиль, а також відхилення потоку акустичної енергії від напрямку хвильового вектора для кристалів $NaBi(MoO_4)_2$.*